Carbon – Science and Technology

Electronic and optical properties of B-N doped carbon nanotubes and graphene: A first principles Study

Debnarayan Jana [(*)] **and Arka Bandyopadhyay**

Department of Physics, University of Calcutta, 92 A.P.C Road, Kolkata-700009, India.
*Author for all correspondence. (E-mail: djphy@caluniv.ac.in)

Abstract: 2D materials as well as quasi-1D materials exhibit fascinating optical and electronic properties. Boron (B) and nitrogen (N) doping are of particular interest due to their expected modification of electronic hence optical properties. We have performed density functional theory (DFT) computations in the low frequency limit to calculate the band structure and dielectric constant of the B-N doped single wall carbon nanotubes (SWCNT) systems. Graphene sheet has been doped with individual B, N atoms along with the simultaneous B-N codoping with varying concentrations. Controllable band gaps have been observed to be induced in the systems for different concentrations of three different foreign species. Besides, the Raman spectrum of the B/N doped Tetragonal graphene (T-graphene) systems has been computed for characterization purpose. Among transition metals, doped in T-graphene system, Sc shows significant spin polarization. Further, the electronic structure and the relevant density of state (DOS) at Fermi energy of B-N doped T-graphene can be judiciously used for the electronic transport. Our theoretical results will serve as an important reference to fabricate various opto-electronic devices with nanoscale dimensions using B/N substitution in the carbon network.

Keywords: Graphene, carbon nanotubes, tetragonal graphene, B-N doping, optical properties, electronic properties. density functional theory (DFT).
----
1. Introduction: Scientific discovery and the technological revolutions strongly depend on materials. Therefore, search of smaller, faster and smarter nano-devices demands the detailed understanding of the properties of different materials to fulfil the need of modern era. In particular, the electronic as well as the optical properties of the nano-systems are not only very importance for basic science but also significant in the industrial applications. The pioneering work of Iijima [1] on the single-walled nanotubes (SWCNTs) [2, 3, 4] inspired the researchers in the field of nanoscience. Several attempts have been made to enhance the efficiency of synthesizing nanotubes and measuring their chemical reactivity [5 - 7]. Moreover, CNTs exhibit profound implementation in the field of molecular electronics [8 - 13], nano-mechanics [14 - 17] and optics [18 - 21]. The electronic states of these CNTs have been efficiently controlled with the help of impurity doping [22 - 24]. Doping carbon nanotubes (CNTs) with different foreign atoms will eventually create new band levels and as a result, a shift in Fermi energy occurs. This shift in Fermi level is the key factor for the electronic including conductivity/magnetic properties of the doped CNTs. However, the most natural choices for foreign atoms have been either boron (B) [25] or N [26], due to three specific reasons. Firstly, B and N are the adjacent atoms of C in the periodic table. Hence, even after the substitution of two C atoms by B-N pair does not alter the number of electrons in the honeycomb lattice of CNT.
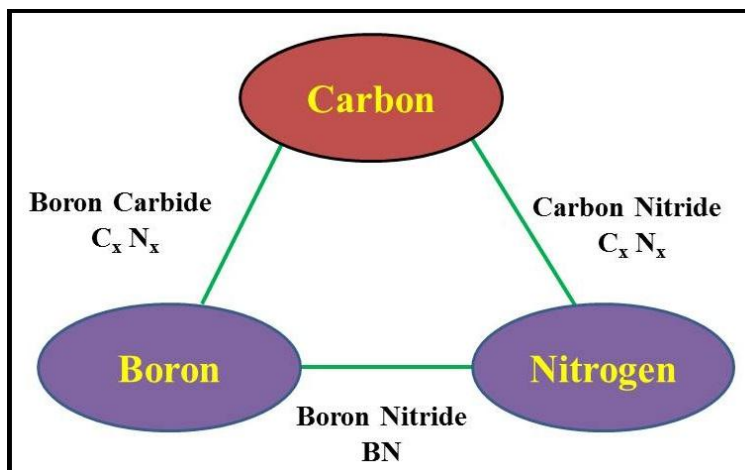
Figure (1): Pictorial representation of possibilities of B and N doping/ alloying.

Secondly, the atomic radius of both B and N closely matches with that of C. Thirdly, it is possible to achieve both p-type and n-type CNTs with appropriate B and N doping. These systems are really important for various device applications. In Figure (1), schematically we depict the different possibilities of B-N alloying in CNT system. The recent developments of two-dimensional (2D) materials in the post-silicon nano-electronics have fostered a magnificent research motivation after the successful isolation of graphene **[27 - 35]**. The rise of each new material leads towards enormous excitements as well as challenges associated with applications of their physical properties. One of the key reasons is that each structure dependent electronic states encompass metallic, semi-metallic, semi-conducting, insulating and superconducting has distinct device applications. These properties of 2D materials are significantly different from their 3D counter parts. Apart from that, there are indeed a class of new novel Dirac materials **[36, 37]** and heterostructures in 2D available either theoretically or experimentally to verify some basic physics along with fabrication of nanodevices. In Figure (2), we schematically present some of the materials possessing Dirac cones.
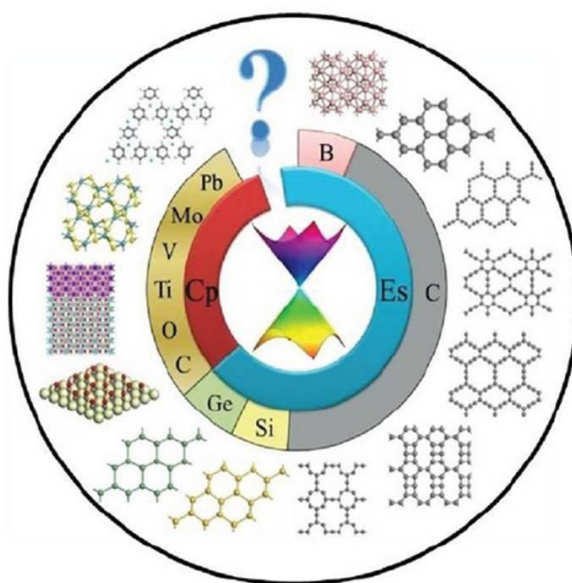

Figure (2): 2D materials with Dirac cones consisting of various elements and compounds. Reproduced from **[37].**

Transition-metal dichalcogenides (TMDCs), another important key member of 2D family also have high potential in device application from the thin films [38] point of view. Furthermore, progress in recent nano-material research has evinced the emergence of different 2D graphene allotropes consist of different hybridizations [39]. Some of them are already experimentally realized [40] within nano dimensions. Tetragonal graphene (T-graphene/TG) [41, 42] (space group P4/mmm) is a prime member of the family of graphene allotropes. This planar allotrope is metallic in nature and comprises squares and octagons made of C atoms. TG has drawn enormous interest of the researchers because of its stability and high DOS at Fermi level [42]. There are many attempts has been made [43 - 47] to functionalize this TG sheet to achieve smart nanoelectronic devices. The incorporation of local symmetry breaking by defects [48], strain engineering, doping, and heterostructuring can tailor the electronic band structure and the optical properties. All the relevant physical properties do depend on the suitable band engineering of these exotic materials. This paper will try to highlight some of the works in the B-N doped carbon system. The B-N doped single walled carbon nanotube (SWCNT) system has been already reviewed by various researchers. We would like to point out the implication of some optical properties based on band structure calculations. Most of the works have been already published but some inherent points are indicated for future devices.
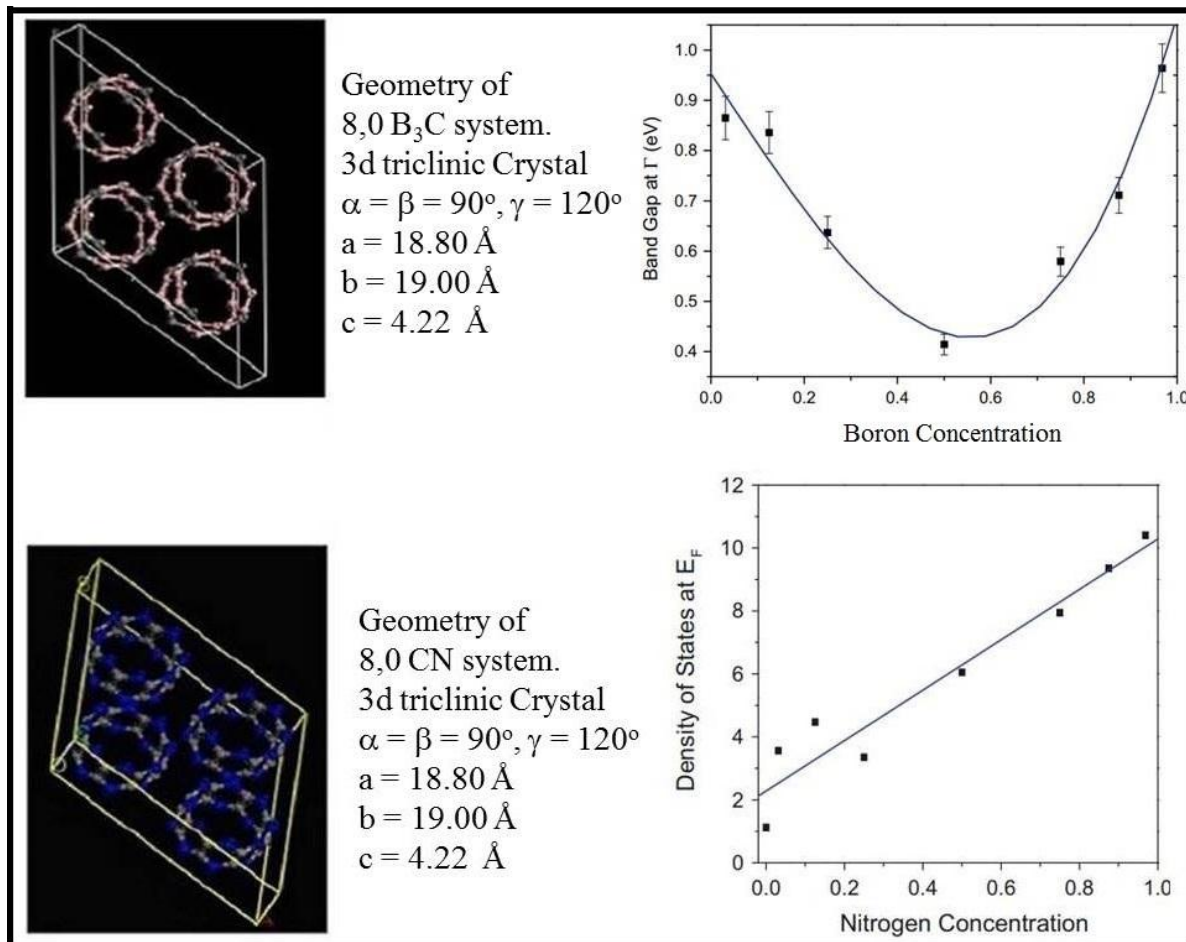

Figure (3): Geometry parameters of (8, 0) B_3C and (8, 0) CN systems, variation of band gap with doping concentration of B atoms and effect of N doping on DOS.

1. B-N doped SWCNT: The B and N doped SWCNTs possess novel electronic and optical properties [24, 25, 26] which have not been observed in pristine Q.CNTs. However, to observe such novel phenomenon, it is essential to have low doping concentration particularly below 0.5%. In fact, it is

necessary to repeat B/N with variable concentration in SWCNTs as well as MWCNTs to understand the relevant mechanism leading to different physical properties. Because of the quasi one dimensional structure of these nanotubes, the size, quantization, flavour along with the position of the doped atoms play the important key factors for the observed novel phenomena in these systems. In Figure (3), we schematically present the geometry of a (8, 0) B_3C system and (8, 0) CN system. It is observed that **[24, 25]**, the B doping can modify the band gap at □ point lies at the centre of the BZ. The band gap reaches the minimum value at about 55% concentration of B. Moreover, N doping can also significantly change the DOS at the Fermi energy. All these results are essential in device fabrication related to CNT. In Table 1 we have highlighted some of the important electronic and optical properties of B alloyed and N alloyed SWCNT system.

A detailed study via DFT has been invoked to probe the interaction of boron with graphite to understand the oxidation mechanism in graphite **[49]**. This work will serve as a benchmark for the study of structural and energetic parameters of boron-graphite system. Recently, codoping CNTs with B and N in the zigzag direction has not shown any effect **[50]** on the bandgap engineering. The BC_2N nanotubes doped with Al and Si atoms **[51]** can be used as a good cathinone drug-sensor with reasonably high sensitivity and low recovery time.

Table 1: Comparison of the opto-electronic properties of B_xC_y and C_xN_y SWCNTs.

Properties	B-alloyed SWCNT	N-alloyed SWNT
Band gap variation at Γ point	Minimum at 55%	Maximum at 57%
Reflectivity	Less	More
Maximum adsorption coefficient	Minimum at 40%	Maximum at 40%
Loss function	Less	More
Plasma frequency	Minimum at 44% (parallel)	Maximum at 50% (paralle)

2. B-N doped graphene: The only drawback of graphene, the wonder material is its zero band gap behaviour at Dirac points. Band gaps can however be induced by various ways such as chemical functionalization, local symmetry breaking with the help of defects and asymmetrical external strain **[52]**. In Figure (4), we depict the B and N doping at various equivalent and non-equivalent sites of graphene network. It is noticed that **[53]**, there are openings of band gap only for non-equivalent sites. Although DFT is a ground state theory, however optical properties with sufficient number of bands can give hints towards the possible excitations of the systems. In Figure (4c), we have compared our DFT results with experimental work **[54]**. Reasonably nice agreement between theory and experiment is noticed.

It has been observed that the edge states of graphene have a significant impact of its electronic properties. The possible approach to achieve such edge effects is reduction of the dimensionality of graphene by making quantum dots (QDs), where the electronic motion is restricted in three spatial directions. Graphene QDs also exhibit extraordinary optoelectronic properties compared to other QDs. In addition, the electronic band spectra can be modified by controlling the shape and size of these quantum dots. Graphene QDs exhibit tunable band gap upto 3 eV which is essential for different optical applications i e. qubits, LEDs, photoresistor, energy conversion bioanalytic sensors, catalysis **[55]** and solar cells **[56]**. Geometrical pattern as well as the concentration of B-N impurity in graphene network **[57 - 59, 53]** and nanoflake **[60]** can significantly modify their electronic properties. For example, increasing the distance between the impurities, it has been established **[60]** that the bandgap and DOS are reduced. It is highly encouraging that most of the 2D materials isolated so far are able to cover the

entire range of the electromagnetic spectrum. B-N pair doping can even open the bandgap in α, β and γ graphynes [61, 62].
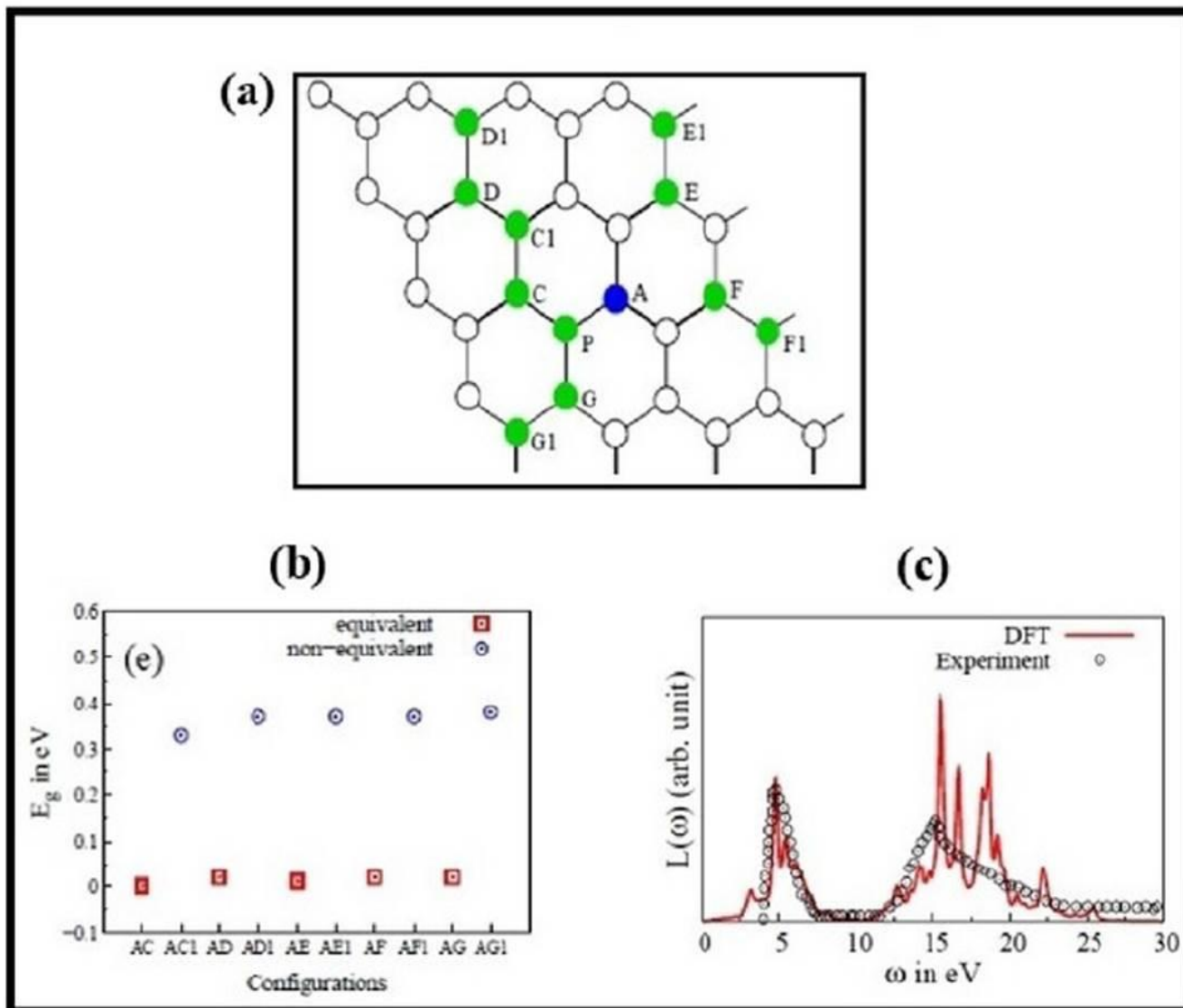

Figure (4): (a) N atom (blue colored) is at A position and B atom (green colored) is successively doped at different equivalent and non-equivelent positions. (b) Variation of band gap equivalent and non-equivalent sites (c) comparison of DFT EELS results with experiment.

In particular, 6,6-12 graphyne nanosheets exhibit extreme sensitivity [63] to light ranging from infrared to UV regime after B-N co-doping. Non-linear behaviour of bandgap opening [64] by suitable controlling the concentration of B/N codoping in graphene has been demonstrated via X-ray emission and emission spectra. The variation of the band gap is restricted to 0.6 eV for the B/N concentration upto 6 %. Further, the behaviour has been explained via DFT computations of a model B-N dopant nanodomains embedded in graphene network. At high enough doping concentration, B-N doped graphene behaves metal-like with zero bandgap. It has been realized that the dopant induced quantum confinement is responsible for the localization of linear dispersive relation. A single step heat treatment method has been applied to synthesize boron and nitrogen doped graphene with the help of PtRu catalysts [65]. The synthesized doped graphene shows an improvement of electrocatalytic performance of methanol oxidation reaction. In particular, the superior catalytic performance is optimized at an annealed temperature of 800 ºC. The role of heteroatoms in doped graphene for photocatalysis has been

critically reviewed by Putri and collaborators [66]. Nitrogen doped graphene has been synthesized by electron beam irradiation and the presence of nitrogen doping at various sites has been morphologically verified [67].
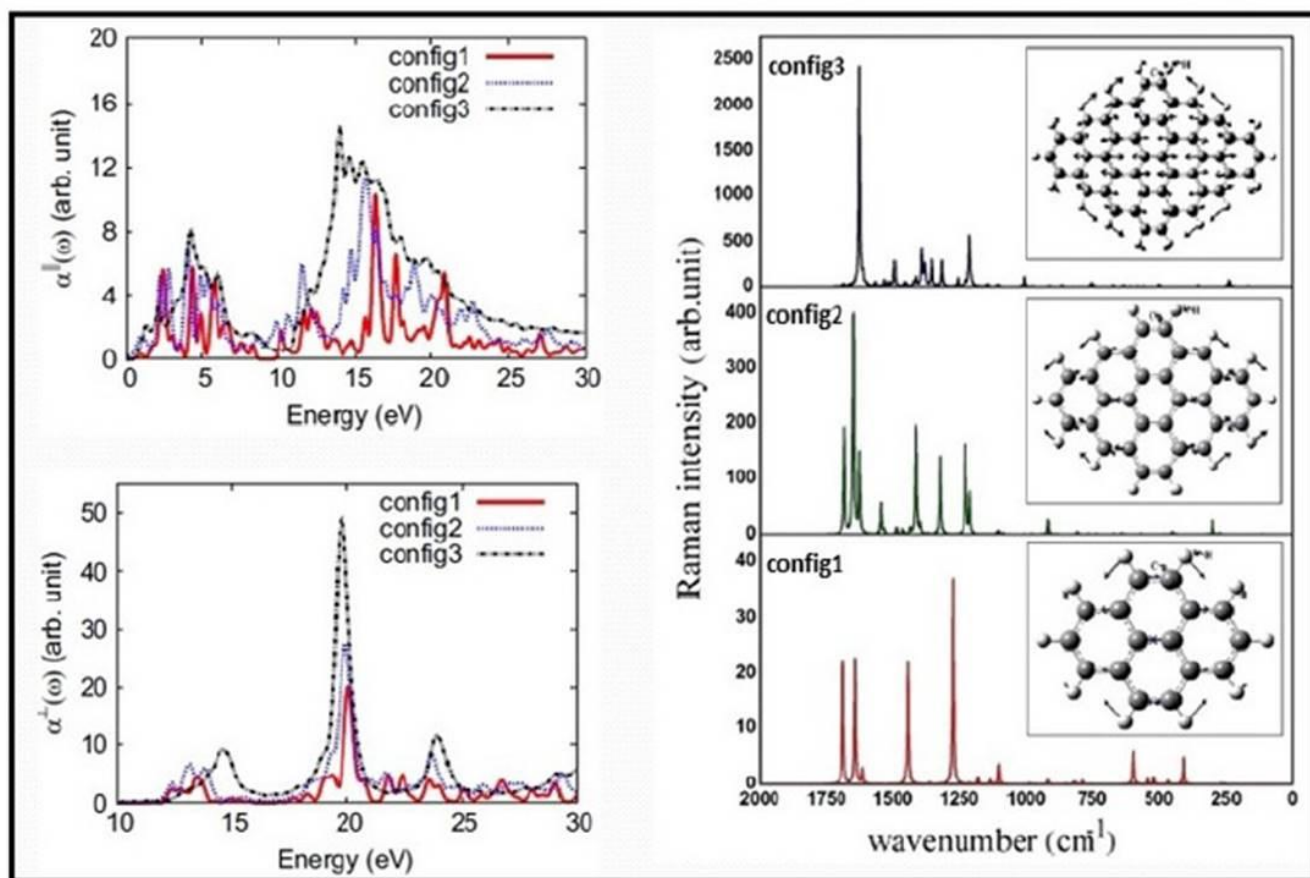

Figure (5): Adsorption coefficient under parallel and perpendicular polarizations and Raman fingerprint of different DSGQDs. Here, config1, config2 and config3 GQDs consist 16, 30 and 48 C atoms respectively.

The enhancement of electrical conductivity along with kinetic performance of supercapacitor has been noticed. The electronic as well as magnetic properties can be altered in graphene network via different substrates such as Si/SiO_2, B-N and transition metal [68]. The absorption of different atoms in the substrate can lead to exotic physical and chemical properties of doped system. In Figure (5), we depict the adsorption coefficient and Raman spectra of three diamond shaped graphene quantum dots (DSGQD) having 16, 30, 48 C atoms for Config 1, Config 2, Config 3 respectively. It is noticed that Config 2 shows peak around 5.35 eV. As size increases, the adsorption spectra become broader [69]. Raman study of H-passivated structures indicates [69] that the intensity and the position along with the nature of vibration change with the cluster size. Based on our result, recently magnetization and magnetic susceptibilities have been computed [70] for diamond shaped graphene quantum dot (DSGQD). In fact, the computational study the magnetic hysteresis of this DSGQD reveals that the magnetic coercivity increases with exchange interaction but decreases with increasing temperature. GQD decorated with flower like rutile TiO_2 can be used [71] for water splitting application. In particular, the optical properties of such GQD having size of 12 nm show high luminescence characteristics and can absorb UV as well as visible light upto 700 nm. The dielectric matrix for parallel as well as perpendicular polarization has been calculated [72] within random phase approximation in DFT. Significant red shift in absorption spectra towards visible range for high B-N co-doping is observed.
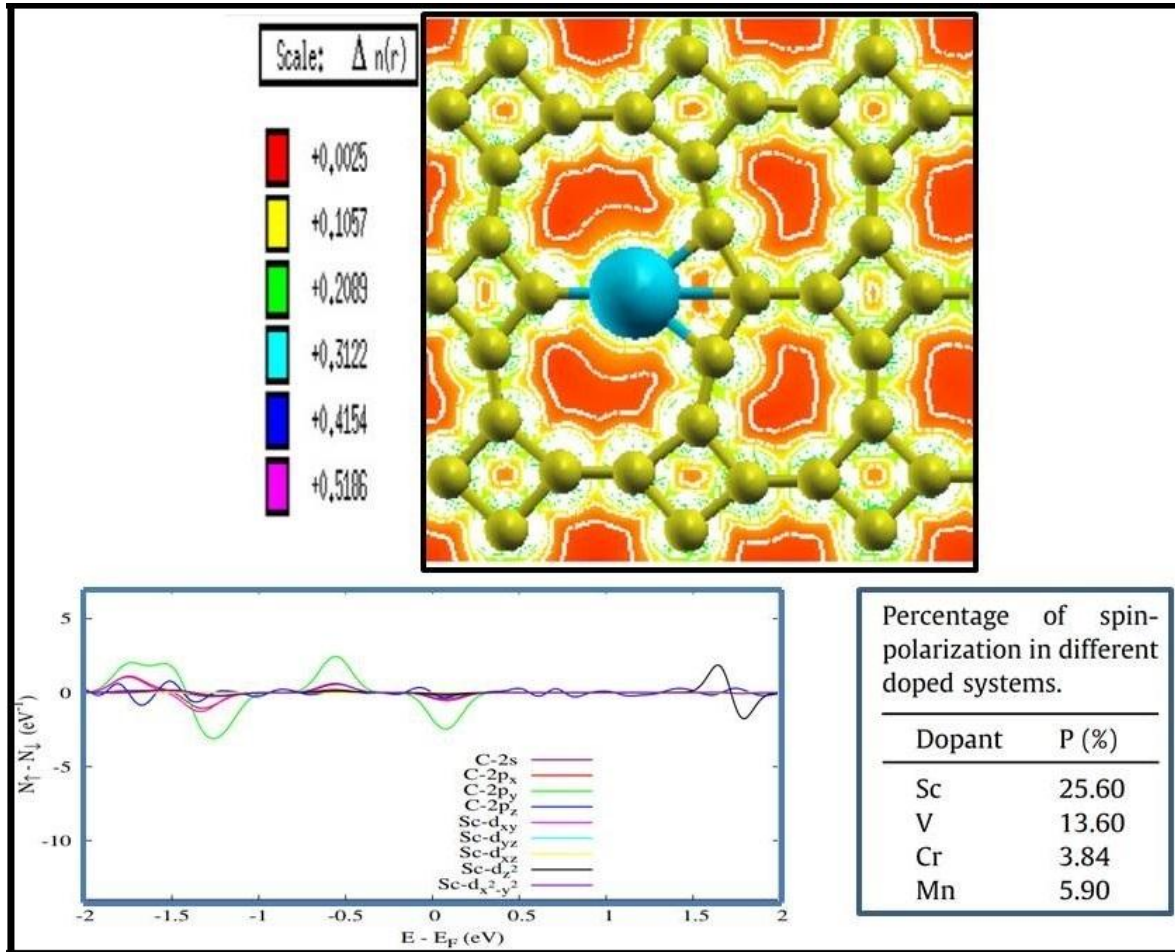
Figure (6): (a) Difference of up spin and down spin DOS of Sc doped planar TG are plotted against energy for various orbitals. (b) Charge density image of Sc doped system. (c) Comparison of percentage of spin polarization at the Fermi energy for various transition metals in TG system.

3. B-N doped T-graphene: In a similar vein to the above discussions, B and N atoms are also natural choices for doping in the T-graphene (TG) network. It is observed that pristine TG is non polar in nature. However, presence of B/N in the TG systems will induce appreciable charge anisotropy in the system. This change in electrical susceptibilities can be perceived from the Raman spectroscopy **[47]**. Projected DOS spectra of transition metal doped TG have been computed via DFT **[46]** and percentage of spin polarization of Sc doped system as a function of energy for various orbitals are shown in Figure (6a). The charge density plot of Sc doped planar TG clearly indicates covalent nature of the bond. The degree of spin polarizations at Fermi energy is defined as shown in equation (1).

$$P = \frac{N_\uparrow(E_F) - N_\downarrow(E_F)}{N_\uparrow(E_F) + N_\downarrow(E_F)} \tag{1}$$

It is clear from the table in Fig. 6(c), the Sc doped planer TG possesses the most spin polarized DOS. Below we have discussed transport phenomenon in B-N doped T-graphene.

4. Methodology: The ballistic transport process is hardly influenced by the resistivity offered by the scattering processes in the molecular sample **[73]**. The conductivity is largely determined by the coupling between the probe and the system. The interaction at the junctions broadens the energy levels and for strong coupling strength the process falls into the self-consistent field (SCF) regime. In the

condition the transport can be calculated in the mean field picture by Landauer formula [73], as shown in equation (2).

$$I = \frac{2e}{h} \int_{-\infty}^{\infty} T(\varepsilon)(f_L(\varepsilon) - f_R(\varepsilon)) d\varepsilon \tag{2}$$

However, the principal contribution is from the orbitals whose energies are compared to that of the Fermi level. Therefore, the effective expression of the current gets modified under external bias V, as shown in equation (3).

$$I(\xi, E_{FM}, V) = \frac{2e}{h} \int_{E_{FM} - \xi eV}^{E_{FM} + (1-\xi)eV} T(\varepsilon) d\varepsilon \tag{3}$$

Here, the voltage division factor (ξ) implies the ratio of the forward (V_f) to reverse (V_r) voltage. It is important to remember that the above expression is only valid at zero temperature limits. However, one can also get some descriptions of the room temperature electron transport. The reason relies on the fact that, the thermal noise is considerably smaller compared to the applied bias in most of the cases. In case of molecule like systems, the exact form of the transmission probability ($T(\varepsilon)$) via a channel of energy ε_0 can be obtained using famous Breit-Wigner formula [74] as shown in equation (4).

$$T(\varepsilon, \varepsilon_0, \alpha, \Gamma_1, \Gamma_2) = \frac{\Gamma_1 \Gamma_2}{(\varepsilon - \varepsilon_0 - \alpha eV)^2 + \frac{(\Gamma_1 + \Gamma_2)^2}{4}} \tag{4}$$

The rates Γ_1 and Γ_2 are related to the imaginary part of self-energy terms ($\Sigma(E) = \Sigma_r(E) + i \Sigma_i(E)$) in non-equlllibrium Green's function formalism as $\Sigma_i(E) = \Gamma_1 + \Gamma_2$. Here, Γ_1 and Γ_2 describes the junction properties of the system. The factor (ξ) is related to the Γ_1 and Γ_2, as $\xi = \Gamma_1 / (\Gamma_1 + \Gamma_2)$. The parameters ε_0 and E_{FM} are taken from the first principles based calculations. The double layer formation at junctions has been considered by introducing a first-order Stark shift like term α in the equation (4).

Γ_1 and Γ_2 depend on applied bias (V), however, $\Gamma_1 (V) + \Gamma_1 (V) = \Gamma_1(0) + \Gamma_1 (0)$ is independent of V, as can be shown in equation (5).

$$\Gamma_1(V) = \Gamma_1(0) + kV \text{ and } \Gamma_2(V) = \Gamma_1(0) - kV \tag{5}$$

here, k is a constant. However the special note is that, this picture is valid for in the SCF regime only. The extension can however be done to encounter the charging effects of a systems [75]. For the time being we will only consider the off-resonance limit in the electron transport process under Wentzel-Kramers- Brillouin (WKB) approximation. With such approximations T-Graphene nanodots have been considered as quantum mechanical tunneling barrier. A detailed description of the measurement process has been shown in Figure (7).
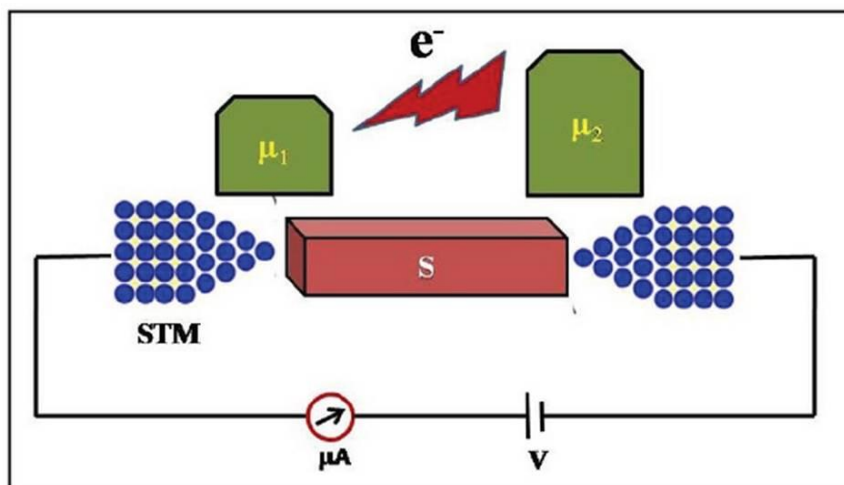
Figure (7): Schematic diagram for I-V measurement using STM tip.

5. Electronic transport of TG clusters: In this section, we will discuss the role of specific substitutional doping sites of B-N pair on electronic transport of TG cluster. We have considered perfectly conducting gold electrodes to evaluate the electro chemical potentials from the DFT calculations. We have chosen square shaped TG clusters with dimension 1 nm x 1 nm to add B-N pair at different sites [76]. It is observed that B-N pair introduces charge anisotropy in the system. Particularly in this work, we have considered two possible orientations of B-N pair possessed maximum dipole moment, as shown in Figure (8). For each configuration, we have further investigated the effect of two different contacts ie, one is in line with the line joining of B-N and another is perpendicular to that. It is interesting to note that, different systems possess different resonance energy of the transmission channels (ε_0) as shown in Table 2.

Table 2: A list of the resonance energy of the transmission channels for A and B systems with contacts in line (par) and perpendicular to the line joining (per) between B and N atoms.

System	ε_0 (eV)
A: par	-4.75
A: per	-5.91
B: par	-4.59
B: per	-4.82

It is observed that each system exhibits diode like behaviour. In Figure (8) two stable configurations of B-N pair exhibit large dipole moments. In addition, the knee voltage of the I-V curve not only varies with doping sites but also with contact positions as depicted in Figure (9). These features can be easily perceived in terms of density of states (DOS) spectra of the systems. Specific sites of B-N pair as well as the contact positions have significant impact on the electronic states near Fermi level (E_F) of the system. It is further observed the structure B respond more to the positions of the contacts compared to A. Sometimes, it is essential to modify the symmetric morphology of the I-V curves for current rectification purpose. In the work we have incorporated the rectifying effect by tuning the parameter α in equation (4). It has been further perceived that conductivity strongly depends on the position of the contact probes. Therefore, we can tune the ratio of the forward and reverse current against particular voltages with the help of α. It can be easily realized that similar to α I-V morphology will also changes with the parameter k.
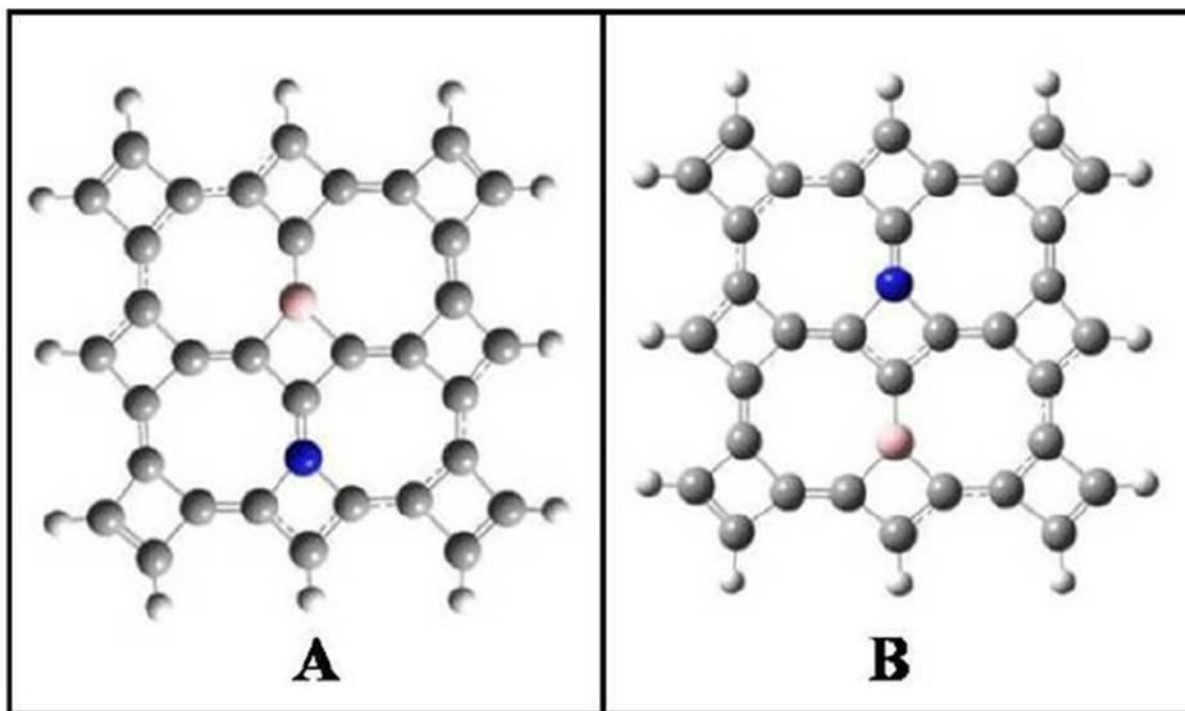
46

Figure (8): Two stable configurations of B-N pair exhibit large dipole moments.
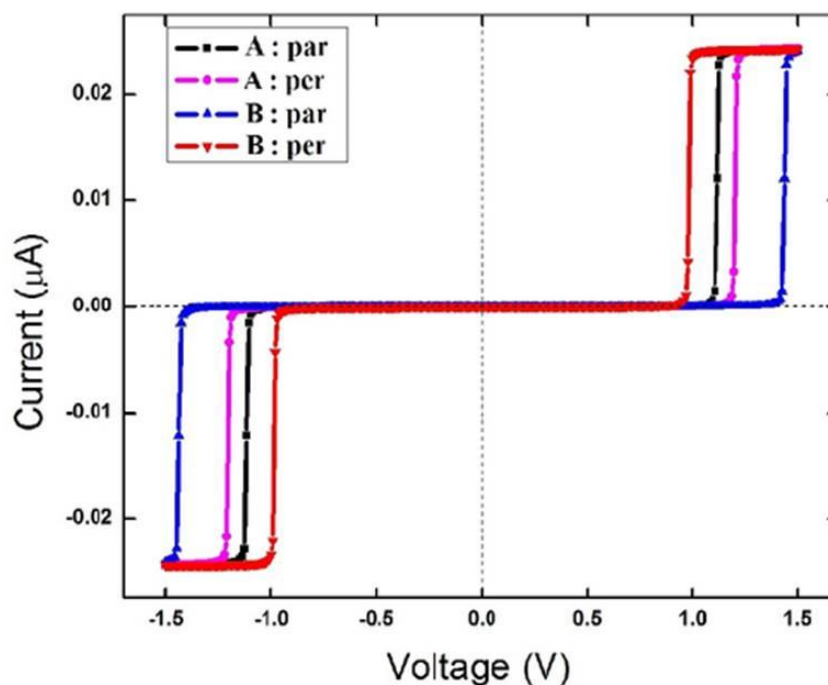

Figure (9): Current-Voltage relationship of the studied configurations.

6. Experimental realization of the model: Despite numerous experimental challenges, I-V nature of C_{60} molecule has been successfully measured using scanning tunnelling microscope (STM) by Joachim and co-workers [77]. They have investigated the I-V nature for different probe system distances. Further, electronics of individual carbon nanotubes and other small scale molecular devices have also been investigated [78, 79]. In recent years, I-V measurements of such small scale systems have been experimentally accomplished by using metallic tip as electrodes for different sample probe distances

[80, 81]. Till then, this method has been supported by many works [82, 83, 84] in the promising field of molecular nano-electronics. It is noteworthy that the systems-probe interactions can be skilfully modified with the help of mechanically controlled break (MCB) junction technique. These experimental developments support our first principles based analytical models to get some idea about the nature of electron transport through such small systems.

7. Conclusions: We have discussed that B-N pair in carbon network can significantly modify the electronic structure and electronic properties. The induced band gaps can be efficiently controlled by changing the concentration as well as the relevant positions in the geometrical network of SWCNT and graphene. From the above discussions it is clear that tetragonal graphene clusters can be used as current rectifiers under suitable conditions. The morphology of I-V curve is largely determined by specific doping sites of B and N because of the structural anisotropy. In addition, positions of probes also influence the electron transport process. For a particular value of first order Stark coefficient like term ($\alpha = 0.5$) the conductivity of the systems has also evaluated. It is observed that the conductivity curve exhibits a sharp peak around the knee voltage. Therefore, with appropriate choices of these external parameters (α and k) electronic orbitals of TG systems can be tuned to get proper current rectification, voltage regulation etc. Thus, it is expected that this study may pave the way of nano-device fabrications involving various functionalized carbon nano-materials.

9. References:

[1]   S. Iijima, Nature 354 (1991) 56.
[2]   R. Saito, G. Dresselhaus, M. S. Dresselhaus, Physical properties of carbon nanotubes (London: Imperial College Press.; 1998).
[3]   S. Reich, C. Thomsen, J. Maulzsch, Carbon nanotubes: basic concepts and physical properties, (Weinheim: Wiley-VCH; 2004).
[4]   W. Zhou, X. Bai, E. Wang, S. Xie, Adv. Mater. 21 (2009) 4565.
[5]   D. Tasis, N. Tagmartarchis, A. Bianco, M. Prato, Chem. Rev. 106 (2006) 1105; See also, R. Weisman, S. Subramoney, Interface 15 (2006) 42.
[6]   P. M. Ajayan. Chem. Rev. 99 (1999) 1787.
[7]   N. Karousis, N. Tagmartarchis, D. Tasis, Chem. Rev. 110 (2010) 5366.
[8]   H. R. Byon, H. C. Choi, J. Am. Chem. Soc. 128 (2006) 2188.
[9]   Z. Chen et al. Science 311 (2006) 1735.
[10]   K. V. Singh et al., Carbon 44 (2006) 1730.
[11]   A. Javey, J. Guo, Q. Wang, M. Lundstrom, H. Dai, Nature 424 (2003) 654.
[12]   P. Avouris. Acc. Chem. Res. 35 (2002) 1026.
[13]   P. R. Bandaru, J. Nanosci. Nanotechnol. 7 (2007) 1.
[14]   D. A. Britz, A. N. Khalobystov, Chem. Soc. Rev. 35 (2006) 637.
[15]   C. Li, T. W. Chou, J. Int. Mater. Syst. Stryc. 17 (2006) 247.
[16]   Y. H. Hun, V. Shanov, M. J. Shultz et al., Smart Mater. Struct. 14 (2005) 1526.
[17]   B. J. Landi et al., Mater. Sci. Eng. B 115 (2005) 359.
[18]   M. Nakazawa et al. Opt. Lett. 31 (2006) 915.
[19]   J. Seo, S. Ma, K. Yang et al. J. Phys: Conf. Ser. 38 (2006) 37.
[20]   Y. Sakakibara, A. G. Rozhin, H. Kataura, Y. Achiba, M. Tokumoto, Jpn. J. Appl. Phys. 44 (2005) 1621.

[21] J. M. Schnorr, T. M. Swager. Chem Mater, 23, 646 (2011).

[22] O. Stephane, P. M. Ajayan, C. Coliex, Ph Redlich, J M Lambert, P. Bernier P, et al. Science, 266, 1683 (1994).

[23] M. Terrones, A. Jorio, A. Endo, A. M. Rao, Y. A. Kim, T. Hayashi et al. Mater Today, 7, 30 (2004).

[24] D. Jana, C. L. Sun, L.-C. Chen and K. H. Chen, Prog. Mater. Sci., 58, 565 (2013).

[25] D. Jana, L. C. Chen, C. W. Chen, S. Chattopadhyay, K. H. Chen, Carbon, 45, 1482 (2007).

[26] D. Jana, A. Chakraborti, L. C. Chen, C. W. Chen, K. H. Chen, Nanotechnology, 20, 175701 (2009).

[27] K. S. Novoselov, A. K. Geim, S. V. Morozov, D. Jiang, Y. Zhang, S. V. Dubonos, I. V. Grigorieva, A. A. Firsov, Science, 306, 666 (2004).

[28] K. S. Novoselov, A. K. Geim, S. V. Morozov, D. Jiang, M. I. Katsnelson, I. V. Grigorieva, S. V. Dubonos, A. A. Firsov, Nature, 438, 197 (2005)

[29] A. Geim, I. Grigorieva. Nature, 499,419 (2013).

[30] A. Gupta, T. Sakthivel, S. Seal, Prog. Mater. Sci., 72, 44 (2015).

[31] Q. Tang and Z. Zhou, Prog. Mater. Sci., 58, 1244 (2013).

[32] Z. S. Butler, S. M. Hollen, L. Cao et al., ACS Nano, 7, 2898 (2013).

[33] G. R. Bhimanapati, Z. Lin, V. Meunier et al., ACS Nano, 9, 11509 (2015).

[34] S. J. Kim, K. Choi, B. Lee, Y. Kim, B. B. Hong Annu. Rev. Mater. Res, 45, 63 (2015).

[35] Z. Lin, A. McCreary, N. Briggs et al., 2D Materials, 3, 042001 (2016).

[36] Z. R. Liu, J. Y. Wang and J. L. Li Phys. Chem. Chem. Phys., 15, 18855 (2013)

[37] J. Wang, S. Deng, Z. Liu, Z. Liu, Nat. Sci. Rev. 2, 22 (2015).

[38] S. J. McDonnell, R. M. Wallace, Thin Solid Films, 616, 482 (2016).

[39] A. N. Enyashin, A. L. Ivanovskii, Phys. Status Solidi B, 248, 1879. (2011).

[40] Y. Li, L. Xu, H. Liu and Y. Li, Chem. Soc. Rev., 43, 2572 (2014).

[41] Y. Liu, G. Wang, Q. Huang, L. Guo and X. Chen, Phys. Rev. Lett. 108, 225505, (2012).

[42] X. Q. Wang, H. D. Li and J. T. Wang, Phys. Chem. Chem. Phys. 14, 11107, (2012).

[43] C. S. Liu, R. Jia, X. J. Ye and Z. Zeng, J. Chem. Phys. 139, 034704, (2013).

[44] X. J. Ye, C. S. Liu, W. Zhong, Z. Zeng and Y. W. Du, J. Appl. Phys., 116, 114304 (2014).

[45] A. Bandyopadhyay, A. Nandy, A. Chakrabarti, D. Jana, Phys. Chem. Chem. Phys, 19, 21584, (2017).

[46] S. Chowdhury, A. Majumder and D. Jana, Journal Magnetism and Magnetic Materials, 441, 523 (2017).

[47] A. Bandyopadhyay, P. Pal, S. Chowdhury and D. Jana, Material Research Express, 2, 095603 (2015).

[48] J. Hong, C. Jin, J. Yuan, Z. Zhang, Adv. Mater., 29, 1606434 (2017).

[49] J. Liu et al., Appl. Surf. Science, 379, 402 (2016).

[50] J. A. Talla and A. A. Ghozlan, Chin. Jour. Phys., 56, 740 (2018).

[51] K. Nejati et al., Jour. Phys. Chem. Solid, 111, 238 (2017).

[52] Y. F. Ziu and Q. Jiang, Cord. Chem. Rev., 326, 1 (2016).

[53] P. Nath, D. Sanyal, D. Jana, Physica E, 56, 64 (2014)

[54] T. Eberlein, U. Bangert, R. R. Nair, R. Jones, M. Gass, A. L. Bleloch et al., Phys Rev B, 77 233406 (2008).

[55] M. Hu, Z. Yao, X. Wang, AIMS Mat. Science, 4, 755 (2017).

[56] P. Bhabhani, Bull. Elec. Eng. Informatics, 7, 42 (2018).

[57] P. Nath, S. Chowdhury, D. Sanyal, D. Jana, Carbon, 73, 275 (2014).

[58] S. Chowhury, R. Das, P. Nath, D. Jana, D. Sanyal, Chemical Functionalization of Carbon Nanomaterials: Chemistry and Applications edited by Vijay Kumar Thakur, Manju Kumari Thakur (CRC Publications, Taylor and Francis, UK, 2015); ISBN: 978-1-4822-5394-8) Pages: 949.

[59] D. Jana, P. Nath and D. Sanyal, Graphene Science Handbook: Nanostructure and Atomic Arrangement, (CRC Publications, Taylor Francis, UK) 231 (2016).

[60] M. H. Mohammed, Physica E, 95, 86 (2018).

[61] J. Yun et al., J. Mater Science, 52, 10294 (2017).

[62] B. Bhattacharya and U. Sarkar, J. Phys. Chem. C, 120, 26793 (2016); B. Bhattacharya, N. B. SIngh, R. Mondal, U. Sarkar, Phys. Chem. Chem. Phys., 17, 19325 (2015).

[63] Z. L. Sun et al, Carbon, 110, 313 (2016).

[64] B. Y. Wang et al., Carbon, 107, 857 (2016).

[65] J. Lu et al., Appl. Surf. Science, 317, 284 (2015).

[66] L. K. Putri et al., Appl. Surf. Science, 358, 2 (2015).

[67] M. Kang, D. H. Lee, J. Yang, Y.-M. Kang and H. Jung, RSC. Adv., 5,104502 (2015).

[68] S. Nigar, Z. Zhou, H. Wang and M. Imtiaz, RSC. Adv., 7, 51546 (2017).

[69] R. Das, N. Dhar, A. Bandyopadhyay, D. Jana, J. Phys Chem. Solid, 99, 34 (2016).

[70] R. Masrour and A. Jabar, Physica A, 497, 211 (2018).

[71] A. Bayat et al., Jour. Energy Chem., 27, 306 (2018).

[72] P. Rani, G. S. Dubey and V. K. Jindal, Physica E, 62, 28 (2014).

[73] S. Datta, 'Electronic Transport in Mesoscopic Systems', Cambridge University Press: New York, (1995).

[74] G. Breit and E. Wigner, Phys. Rev. 49, 519 (1936).

[75] H. A. Cabrera-Tinoco, A. C. L. Moreira and C. P. de Melo, J. Phys. Chem, 148, 194304 (2018).

[76] A. Bandyopadhyay, S. Paria, D. Jana, J. Phys. Chem. Solids 123, 172(2018).

[77] C. Joachim, J. K. Gimzewski, R. R. Schlitter, and C. Chavy, Phys. Rev. Lett., 74, 2102, (1995).

[78] T. W. Ebbesen, H. J. Lezec, H. Hiura, J. W. Bennett, H. F.Ghaemi, and T. Thio, Nature, 382, 54, (1996).

[79] M. A. Reed, C. Zhou, C. J. Muller, T. P. Burgin and J. M. Tour, Science, 278, 252, (1996).

[80] J. Reichert, R. Ochs, D. Beckmann, H. B. Weber, M. Mayor and H. V. Lohneysen, Phys. Rev. Lett., 88, 176804 (2002).

[81] C. Kergueris, J. P. Bourgoin, S. Palacin, D. Esteve, C. Urbina, M. Magoga and C. Joachim, Phys. Rev. B, 59, 505 (1999).

[82] B. Capozzi, J. Z. Low, J. X., Z. F. Liu, J. B. Neaton, L. M. Campos and L. Venkataraman, Nano Lett, 16, 3949 (2016).

[83] M. L. Perrin, E. Gal_an, R. Eelkema, J. M. Thijssen, F. Grozemab and H. S. J. van der Zant, Nanoscale, 8, 8919, (2016).

[84] Z. F. Liu and J. B. Neaton, J. Phys. Chem. C, 121, 21136 (2017).

*****